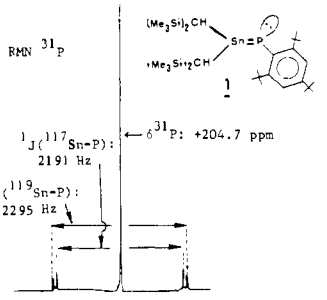

Figure 1.

2 was synthesized by addition of the lithiophosphine 3 (prepared by reacting *n*-butyllithium (1.6 M in hexane) with (2,4,6-*tert*-butylphenyl)phosphine (4) in diethyl ether) to bis[bis(trimethylsilyl)methyl]difluorotin (5)[9,10] (eq 1).

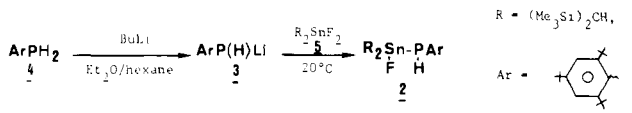

(1)

Addition of 1 equiv of *t*-BuLi to 2 in THF solution was performed at −50 °C. On warming to room temperature a red color developed; after centrifugation of lithium fluoride and removal of solvents under vacuum, we obtained an air-sensitive red crystalline crude material. NMR analysis showed the formation of stannaphosphene 1 as the major product (relative percentage 70%); as minor products we have characterized the secondary phosphine 6[11] (20%), the disecondary diphosphine 7[12] (5%), and the stannylene 8[13] (5%). The probably radical process leading to 6–8 is not yet completely elucidated and its study is now under investigation (eq 2).

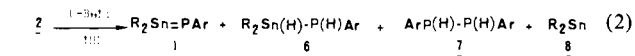

(2)

The stannaphosphene structure of 1 was unambiguously determined by ^1H, ^{31}P, ^{119}Sn NMR (see Figure 1) and by mass spectroscopy. ^1H NMR data (solvent C_6D_6) are as follows: δ 0.25 (s, 18 H, Me_3Si), 0.38 (s, 18 H, Me_3Si), 1.43 (s, 9 H, p-*t*-Bu), 1.78 (s, 18 H, o-*t*-Bu), 7.43 (d, 2H, $^4J_{PH}$ = 2.5 Hz, ArH). The ^{31}P NMR chemical shift of 1 (+204.7 ppm/H_3PO_4) falls in the range of the known silaphosphene[5] (+136.0 ppm) and germaphosphene[6] (+175.4 ppm). More significant is the coupling constant between phosphorus and tin: $^1J_{P-^{117}Sn}$ = 2191 Hz, $^1J_{P-^{119}Sn}$ = 2295 Hz. These values, much larger than for single-bonded tin–phosphorus compounds (e.g., 1150 and 1203 Hz respectively in 2), can be attributed to a π-bond between tin and phosphorus. A similar effect has been observed in the coupling constants $^1J_{P-^{29}Si}$ in silaphosphene[5] and $^1J_{PP}$ in diphosphenes.[1] The ^{119}Sn chemical shift, falling at very low field (+658.3 ppm/Me_4Sn)[14] is the first NMR data for tricoordinate, p–π hybridized tin.[15,16] The electronic spectrum of 1 (THF, pentane) exhibits peaks at λ_{max} 460 ($n \rightarrow \pi^*$) and 350 nm ($\pi \rightarrow \pi^*$). Mass spectrum presents a parent peak at *m/e* 714 (^{120}Sn); experimental peak patterns were assigned after comparison with calculated theoretical peak patterns. Thermal stability of 1 is rather good; it persits for a week at room temperature.

The structure of 1 was corroborated by its chemical behavior. Reactivity of 1 is very high toward compounds with active hydrogens, e.g., methanol and hydrogen chloride, which add to the tin–phosphorus double bond; these highly regiospecific reactions, performed at room temperature in pentane, confirm the expected polarity of the Sn=P bond with tin as the more positive partner leading respectively to the secondary phosphines 9[17] and 10[18] in nearly quantitative yields. Reduction of 1 by $LiAlH_4$ affords 6[11] (eq 3).

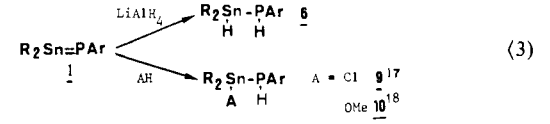

(3)

Chemical and physicochemical aspects of the tin–phosphorus double bond of 1 are under active investigation.

(9) 5 has been prepared by fluorination of $[(Me_3Si)_2CH]_2SnCl_2$[10] with KF/EtOH/H_2O at 40 °C for 2 h and recrystallized from pentane to afford white needles: mp 113–116 °C; ^1H NMR (C_6D_6) δ 0.25 (s, 18 H, Me_3Si); $^{119}Sn\{^1H\}$ NMR (C_6D_6) δ −18.1 (t, $^1J_{SnF}$ = 3042 Hz); ^{19}F NMR (C_6D_6) δ −86.3. Anal. Calcd for $C_{14}H_{38}F_2Si_4Sn$: C, 35.36; H, 8.06; F, 7.99. Found: C, 35.45; H, 8.11; F, 8.05.

(10) Fjeldberg, T.; Haaland, A.; Lappert, M. F.; Schilling, B. E. R.; Seip, R.; Thorne, A. J. *J. Chem. Soc., Chem. Commun.* **1982**, 1407–1408.

(11) 6 has been prepared in an independent synthesis by reduction of 9 with $LiAlH_4$ in Et_2O: ^1H NMR (C_6D_6) δ 0.30 (br s, 36 H, Me_3Si), 1.33 (s, 9 H, p-*t*-Bu), 1.73 (s, 18 H, o-*t*-Bu), 7.47 (d, 2 H, Ar H, $^4J_{PH}$ = 2.5 Hz); ^{31}P (C_6D_6) δ −129.7, $^1J_{PH}$ = 201.7, $^2J_{PH}$ = 12.0, $^1J_{P-^{117}Sn}$ = 755.9, $^1J_{P-^{119}Sn}$ = 791.2 Hz; IR ν(PH) 2383, ν(SnH) 1826 cm^{-1}. Anal. Calcd for $C_{32}H_{69}PSiSn$: C, 53.68; H, 9.71. Found: C, 53.89; H, 9.98.

(12) Cowley, A. H.; Kilduff, J. E.; Newman, T. H.; Pakulski, M. *J. Am. Chem. Soc.* **1982**, *104*, 5820–5821.

(13) Davidson, P. J.; Lappert, M. F. *J. Chem. Soc., Chem. Commun.* **1973**, 317–318.

(14) Silenes, disilenes, and silaphosphenes exhibit, for the tricoordinate, p–π hybridized silicon, low-field ^{29}Si chemical shifts;[1] the δ ^{119}Sn of 1 is in good agreement with Si/Sn chemical shifts correlations: Watkinson, P. J.; MacKay, K. M. *J. Organomet. Chem.*, **1984**, *275*, 39–42.

(15) Until now, only one compound, the distannene $[(Me_3Si)_2CH]_2Sn{=}Sn[CH(SiMe_3)_2]_2$ has been reported to have a tin–tin double bond in the solid phase.[16] But in solution this compound gives the two stannylenes $[(Me_3Si)_2CH]_2Sn$.[13]

(16) Goldberg, D. E.; Harris, D. H.; Lappert, M. F.; Thomas, K. M. *J. Chem. Soc., Chem. Commun.* **1976**, 261–262.

(17) 9 has been prepared independently from $[(Me_3Si)_2CH]_2SnCl_2$ and 3: white crystals, mp 158 °C; ^1H NMR (C_6D_6) δ 0.23 (br s, 36 H, Me_3Si), 1.23 (s, 9 H, p-*t*-Bu), 1.60 (s, 18 H, o-*t*-Bu), 7.37 (d, 2 H, $^4J_{PH}$ = 2.2 Hz, Ar H); ^{31}P NMR (C_6D_6) δ −100.3, $^1J_{PH}$ = 195.3, $^1J_{P-^{117}Sn}$ = 1253.1, $^1J_{P-^{119}Sn}$ = 1297.2 Hz. Anal. Calcd for $C_{32}H_{68}ClPSiSn$: C, 51.22; H, 9.13; Cl, 4.72. Found: C, 50.88; H, 9.02; Cl, 4.88.

(18) 10 has been prepared independently by reaction between 2 and MeOLi at 90 °C in a sealed tube: ^1H NMR (C_6D_6) δ 0.27 (br s, 36 H, Me_3Si), 1.30 (s, 9 H, p-*t*-Bu), 1.68 (s, 18 H, o-*t*-Bu), 3.87 (s, 3 H, OMe), 7.53 (d, 2 H, Ar H, $^4J_{PH}$ = 2.2 Hz); ^{31}P (C_6D_6) δ −116.0, $^1J_{PH}$ = 205.3, $^1J_{P-^{117}Sn}$ = 1053.0, $^1J_{P-^{119}Sn}$ = 1103.0 Hz; mass spectroscopy (desorption) 746 (^{120}Sn, M).

Novel Structure of the Complex between Carboxypeptidase A and a Ketonic Substrate Analogue

David W. Christianson,† Lawrence C. Kuo,‡ and William N. Lipscomb*

Gibbs Chemical Laboratories
Department of Chemistry, Harvard University
Cambridge, Massachusetts 02138
Received July 19, 1985

As part of a continuing series of high-resolution X-ray crystallographic studies of the interaction of inhibitors with the zinc metalloprotease carboxypeptidase A_α (CPA),[1,2] we report the structure of the complex between CPA and the substrate analogue

† AT&T Bell Laboratories Scholar.
‡ Fellow of the Jane Coffin Childs Memorial Fund for Medical Research. Current address: Department of Chemistry, Boston University, Boston, MA 02115.

(1) For some recent reviews of CPA, see: (a) Lipscomb, W. N. *Proc. Natl. Acad. Sci. U.S.A.* **1980**, *77*, 3875–3878. (b) Lipscomb, W. N. *Acc. Chem. Res.* **1982**, *15*, 232–238. (c) Lipscomb, W. N. *Annu. Rev. Biochem.* **1983**, *52*, 17–34. (d) Vallee, B. L.; Galdes, A.; Auld, D. S.; Riordan, J. F. In "Metal Ions in Biology"; Spiro, T. G., Ed.; Wiley: New York, 1983; Vol. 5, pp 25–75. (e) Vallee, B. L.; Galdes, A. *Adv. Enzymol.* **1984**, *56*, 283–430.

(2) (a) Lipscomb, W. N.; Hartsuck, J. A.; Reeke, G. N., Jr.; Quiocho, F. A.; Bethge, P. H.; Ludwig, M. L.; Steitz, T. A.; Muirhead, H.; Coppola, J. *Brookhaven Symp. Biol.* **1968**, *No. 21*, 24–90. (b) Rees, D. C.; Honzatko, R. B.; Lipscomb, W. N. *Proc. Natl. Acad. Sci. U.S.A.* **1980**, *77*, 3288–3291. (c) Rees, D. C.; Lipscomb, W. N. *Proc. Natl. Acad. Sci. U.S.A.* **1980**, *77*, 4633–4637. (d) Rees, D. C.; Lipscomb, W. N. *Proc. Natl. Acad. Sci. U.S.A.* **1981**, *78*, 5455–5459. (e) Rees, D. C.; Lipscomb, W. N. *J. Mol. Biol.* **1982**, *160*, 475–498. (f) Christianson, D. W.; Lipscomb, W. N. *Proc. Natl. Acad. Sci. U.S.A.* **1985**, *82*, 6840–6844.

0002-7863/85/1507-8281$01.50/0

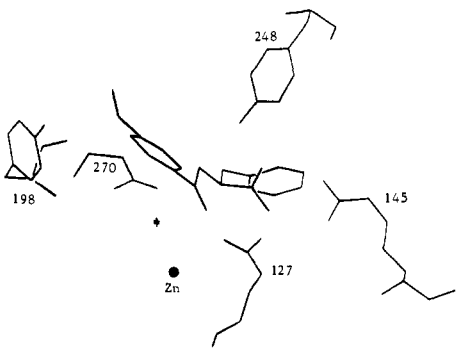

Figure 1. BMBP bound to the active site of CPA. Enzyme residues, in clockwise direction starting with Zn, are Tyr-198, Glu-270, Tyr-248, Arg-145, and Arg-127. The zinc-bound water molecule is depicted as a star.

(−)-3-(*p*-methoxybenzoyl)-2-benzylpropanoic acid (BMBP)[3] at 1.54-Å resolution. Although a structural study of this complex has been reported at 2.8-Å resolution,[2b] the higher resolution data have yielded a well-resolved structure in which the binding site of the carbonyl oxygen is different from that interpreted from the difference electron density maps calculated against the native enzyme at lower resolution. Crystals of the CPA–BMBP complex were prepared as previously documented,[2b] and data to 1.54-Å resolution were collected on a Syntex $P2_1$ diffractometer and reduced[4] as described.[2f] The model[5] was refined[6] against the data to a final crystallographic *R* factor[7] of 0.186 at 1.54-Å resolution.[8]

The BMBP molecule makes most of the usual contacts observed in CPA–inhibitor complexes: the benzyl group resides in the hydrophobic pocket of the enzyme, and the carboxylate moiety forms a salt link with the guanidinium group of Arg-145. Tyr-248 is in the "down" position, and its phenolic oxygen forms a hydrogen bond (2.4 Å) with a carboxylate oxygen of BMBP. Tyr-198 also forms a long hydrogen bond (within experimental error at 3.4 Å) with the methoxybenzoyl group of the inhibitor. However, the carbonyl oxygen corresponding to the scissile carbonyl of an actual substrate is *not* coordinated to the zinc ion as previously reported (the oxygen–zinc distance is 3.9 Å); instead, it accepts a bifurcated hydrogen bond (2.9 Å to each terminal nitrogen) from the guanidinium moiety of Arg-127. Interestingly, the carbonyl oxygen of the dipeptide Gly-Tyr is observed to receive a hydrogen bond from Arg-127 in its complex with the apoenzyme,[9] whereas in the holoenzyme it is coordinated to the zinc ion.[2a,10] Arg-127 also hydrogen bonds (3.1 Å) to a carboxylate oxygen of BMBP, an interaction also observed in another recent enzyme–inhibitor structure.[2f] Hence, Arg-127 is now implicated as a residue important for the binding of certain inhibitors and possibly substrates, products, and transition states to the active site of CPA. The zinc-bound water remains on the zinc in the CPA–BMBP complex, and enzyme residues serving as zinc ligands (His-69, His-196, and Glu-72) show no conformational changes upon the binding of the inhibitor. A diagram showing the inhibitor with relevant enzyme residues is presented in Figure 1, and pertinent electron density maps are presented in Figure 2.

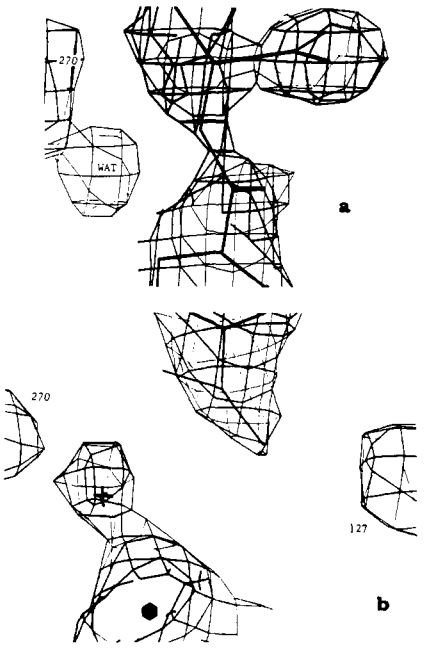

Figure 2. (a) Portion of a $(5|F_o| - 4|F_c|)$ difference electron density map looking down along the carbonyl of BMBP. Structure factors were calculated from the native enzyme refined at 1.54-Å resolution, omitting active-site water molecules. Atomic coordinates are superimposed on the map, and density corresponding to Glu-270 and the zinc-bound water is indicated. The water molecule is 3.1 Å and the carboxylate oxygens of Glu-270 are 4.5 and 5.0 Å away from the BMBP carbonyl carbon. (b) Same map as (a) but viewed at a different angle. Glu-270 and Arg-127 are indicated; the zinc ion and water molecule are represented by a hexagon and star, respectively.

The mode of binding of BMBP is consistent with several mechanisms, including both the anhydride pathway proposed for ester hydrolysis[11] and the general base pathway. Additionally, proposed roles for Arg-127 as a hydrogen bond donor[1b,2f] in either mechanistic pathway are supported by the observed interactions. Nevertheless, the binding mode of BMBP to CPA may display the potential of resolving differences between the behavior of various substrates, such as peptides and certain esters.[1d,e,12] Whatever the differences, either mode of binding of the carbonyl oxygen (to zinc or Arg-127) maintains the integrity of the current structural assignments of enzyme subsites S_1' and S_1. One possible hypothesis, consistent with much current structural and chemical evidence, is that as S_1' and S_1 become occupied, the carbonyls of certain esters may initially bind to zinc while those of peptides initially bind to Arg-127. The dipeptide Gly-Tyr could preferentially bind to zinc solely by virtue of a favorable chelate interaction supplied by both the carbonyl oxygen and the free terminal amino group.

It has been shown[3] that CPA catalyzes the stereospecific exchange of one of the methylene protons of BMBP. In view of the structure of what should be an actively exchanging complex, it is hard to designate the catalytically responsible residue(s). The carboxylate oxygens of Glu-270 are 3.5 and 4.5 Å from the methylene carbon; the zinc-bound water is closer (3.2 Å), but in poor geometric orientation for exchange. Given the temporal

(3) (a) Sugimoto, T.; Kaiser, E. T. *J. Am. Chem. Soc.* **1978**, *100*, 7750–7751. (b) Sugimoto, T.; Kaiser, E. T. *J. Am. Chem. Soc.* **1979**, *101*, 3946–3951.

(4) The *R* factor for scaling and merging the data obtained from three crystals was 0.060, where

$$R = \sum|I_{hi} - \langle I_h\rangle|/\sum\langle I_h\rangle$$

I_{hi} = scaled intensity for reflection *h* in data set i; $\langle I_h\rangle$ = average intensity calculated for reflection *h* from replicate data.

(5) Model building was performed on an Evans and Sutherland PS300 interfaced with a VAX 11/780, with graphics software developed by Jones as modified by Pflugrath and Saper (FRODO); see: Jones, T. A. In "Computational Crystallography"; Sayre, D., Ed.; Oxford Univ Press: London, 1982; pp 303–317.

(6) A reciprocal space stereochemically restrained least-squares algorithm was utilized in protein refinement; see: Hendrickson, W. A.; Konnert, J. In "Biomolecular Structure, Function, Conformation, and Evolution"; Srinivasan, R., Ed.; Pergamon: London, 1981; Vol. 1, pp 43–47.

(7) $R = \sum||F_o| - |F_c||/\sum|F_o|$.

(8) An rms error in atomic positions was estimated to be about 0.2 Å on the basis of relationships derived by Luzzati; see: Luzzati, V. *Acta Crystallogr.* **1952**, *5*, 802–810.

(9) Rees, D. C.; Lipscomb, W. N. *Proc. Natl. Acad. Sci. U.S.A.* **1983**, *80*, 7151–7154.

(10) Rees, D. C.; Lewis, M.; Honzatko, R. B.; Lipscomb, W. N.; Hardman, K. D. *Proc. Natl. Acad. Sci. U.S.A.* **1981**, *78*, 3408–3412.

(11) (a) Kuo, L. C.; Makinen, M. W. *J. Biol. Chem.*, **1982**, *257*, 24–27. (b) Kuo, L. C.; Makinen, M. W. *J. Am. Chem. Soc.* **1985**, *107*, 5255–5261.

(12) See: Breslow, R.; Wernick, D. *Proc. Natl. Acad. Sci. U.S.A.* **1977**, *74*, 1303–1307 and references therein.

resolution inherent in X-ray crystallographic data collection, another low-occupancy conformation of Glu-270 and/or the zinc-bound water, or BMBP itself, may effect the kinetically slow exchange, resulting in a time-averaged structure showing little or no sign of such an alternate conformation.

Acknowledgment. We thank the National Institutes of Health for Grant GM 06920 in support of this research and the National Science Foundation for Grant PCM-77-11398 for support of the computational facility. We thank Patricia Christianson for her help with the figures, the Jane Coffin Childs Memorial Fund for Medical Research for a postdoctoral fellowship to L.C.K., and AT&T Bell Laboratories for a doctoral fellowship to D.W.C.

A Quantitative Theory of Mass Spectral Fragmentation Patterns

J. Silberstein and R. D. Levine*

The Fritz Haber Research Center for Molecular Dynamics, The Hebrew University Jerusalem 91904, Israel

Received July 30, 1985

The discovery of laser-pumped multiphoton ionization–fragmentation[1,2] led to renewed interest in the dissociation processes of energy-rich polyatomic ions. Often, the laser pulse is long enough in time to allow absorption of light by fragment ions.[1,3-5] A simpler process is thus fragmentation induced by electron impact where all the available energy is deposited in the parent molecular ion. Any theory of the fragmentation pattern should thus work for mass spectral patterns. Yet even on a qualitative level the observed mass spectrum for electron impact is different than the laser-induced one. The latter pattern can be varied, often from a very soft ionization producing mostly the parent to very extensive fragmentation, by increasing the laser power. In an attempt to interpret such observations, we have proposed[6] that the fragmentation pattern is governed primarily by the mean energy, $\langle E \rangle$, absorbed per parent molecule. This has indeed been verified.[7,8] Yet such an assumption (which is part also of the more detailed mechanistic approach[9]) leads to a very characteristic qualitative behavior of the predicted fragmentation pattern. At very low values of $\langle E \rangle$ (measured from the ground state of the parent ion), one obtains mostly the parent itself. As $\langle E \rangle$ is increased, the spectrum consists of primary dissociation products. At high $\langle E \rangle$ values the spectrum consists mostly of "energy expensive" products. Such multiphoton ionization fragmentation patterns where the parent as well as energy expensive ions are present is interpreted in the mechanistic approach[9] as due to selective absorption of energy by secondary ions. Indeed, for short laser pulses[10] the mass spectrum is "narrower". Electron impact fragmentation typically produces little of the energy expensive ions. Otherwise, however, it spans a wider mass range, showing simultaneously both low and intermediate energy product ions.

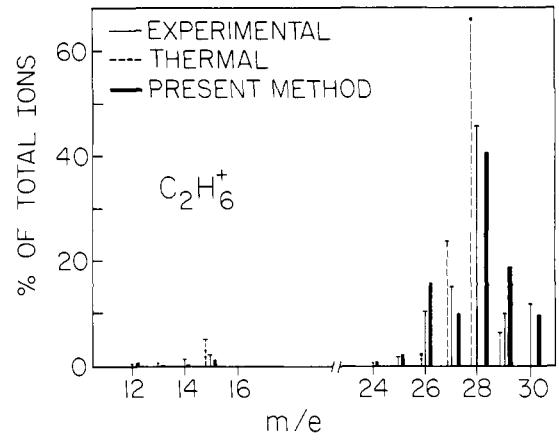

Figure 1. Measured[12] electron impact mass spectrum off ethane and two sets of computational results: (i) a computation based on specifying just the mean energy, $\langle E \rangle$, of excitation per parent molecule. This leads to a thermallike distribution $f(E)$ of the excitation energy. We have used that value of $\langle E \rangle$ that best fits the observed spectrum ($\langle E \rangle$ = 4.3 eV above the ground state of $C_2H_6^+$). (ii) Results obtained by using a wider distribution of energy with $\langle E \rangle$ = 5.7 eV.

The computational procedure[9] is to determine the branching fractions into all possible dissociation channels of the parent ion. This is done by seeking that set of branching fractions which is of maximal entropy subject to constraints. It is the constraints that specify the nature of the process. The simplest constraint and one that works well for laser-induced processes is to specify the mean energy, $\langle E \rangle$, absorbed per parent molecule. The final answer is then remarkably simple.[9] The branching fraction for any dissociation pathway of the parent ion is fully determined as a product of relevant partition functions. As a concrete example consider computing the fragmentation pattern of $C_2H_6^+$. The branching fraction for, say, the $C_2H_6^+ \rightarrow C_2H_4^+ + H_2$ reaction is given by

$$q = Q_{C_2H_4^+} Q_{H_2} Q_T / N \qquad (1)$$

Q_X is the partition function for molecule X, here X is $C_2H_4^+$ or H_2 and Q_T is the partition function for the relative translational motion of the fragments. N is the normalization constant such that the sum of branching fractions for all possible dissociation processes is unity.

The fragmentation pattern can therefore be computed using standard thermochemical data of stable species[11] without adjustable parameters. The value of the temperature at which the partition functions are to be evaluated is that which reproduces the mean energy $\langle E \rangle$ per parent molecule. This approach works reasonably well for multiphoton excitation but fails, Figure 1, to provide a quanitative agreement for electron impact mass spectra. The primary deficiency, as seen in Figure 1 and in other cases as well, is that when $\langle E \rangle$ is chosen so as to provide the best possible fit to the observed spectrum, hardly any undissociated parent survives.

The maximum entropy formalism determines the energy distribution in the energy-rich parent ion from the given value of $\langle E \rangle$. We here consider the possibility that the resulting distribution for electron impact excitation is too narrow. To broaden the theoretical distribution one needs to specify additional moments of the distribution besides $\langle E \rangle$. Once that is done, the agreement with the electron impact fragmentation pattern[12] becomes quantitative, Figure 1.

The important practical point is that even when additional moments of the energy distribution are specified the branching fraction can still be computed from the densities of states of the

(1) Schlag, E. W.; Neusser, H. J. *Acc. Chem. Res.* **1983**, *16*, 355.
(2) Bernstein, R. B. *J. Phys. Chem.* **1982**, *86*, 1178.
(3) Durant, J. L.; Rider, D. M.; Anderson, S. L.; Proch, F. D.; Zare, R. N. *J. Chem. Phys.* **1984**, *80*, 1817.
(4) Koplitz, B. D.; McVey, J. K. J. *Chem. Phys.* **1984**, *80*, 2271.
(5) Stiller, S. W.; Johnston, M. V. *J. Phys. Chem.* **1985**, *89*, 2717.
(6) Silberstein, J.; Levine, R. D. *Chem. Phys. Lett.* **1980**, *74*, 6. Silberstein, J.; Levine, R. D. *J. Chem. Phys.* **1981**, *75*, 5735.
(7) Lichtin, D. A.; Bernstein, R. B.; Newton, K. R. *J. Chem. Phys.* **1981**, *75*, 5728.
(8) Lubman, D. M. *J. Phys. Chem.* **1981**, *85*, 3752.
(9) Silberstein, J.; Levine, R. D. *Chem. Phys. Lett.* **1983**, *99*, 1; *J. Phys. Chem.*, in press.
(10) Gobeli, D. A.; Simon, J. D.; El-Sayed, M. A. *J. Phys. Chem.* **1981**, *88*, 3949.
(11) Rosenstock, H. M.; Draxl, K.; Steiner, D. W.; Herron, J. T. *J. Phys. Chem. Ref. Data, Suppl.* **1977**, *6*, (1).
(12) Mass Spectral Data, American Petroleum Institute, Research Project 44, Carnegie Institute of Technology, Pittsburgh, PA, 1955.

0002-7863/85/1507-8283$01.50/0